

The Effects of Magnetic Field on Boundary Layer Nano-fluid Flow Over Stretching Sheet

Emad M. Abo-Eldahab¹, Rasha Adel¹, Hoda M. Mobarak¹ and M. Abdelhakem^{1,2,*}

¹Department of Mathematics, Faculty of Science, Helwan University, Cairo, Egypt

²Basic Science Department, School of Engineering, Canadian International College, New Cairo, Egypt

Received: 21 Feb. 2021, Revised: 22 June 2021, Accepted: 26 June 2021

Published online: 1 Nov. 2021

Abstract: The effects of magnetic field on boundary layer nano-fluid flow over stretching sheet have been investigated. Different factors affecting the nano-fluid's motion and particles have been studied, mainly the changes in the stretching sheet caused by an external magnetic field with nano-particles such as Cu. Therefore, we modified and improved a model to study boundary layers nano-fluid flow. That model's partial differential equations (PDEs) will be transformed into a non-linear higher-order system of ordinary differential equations (h-order ODEs) using similarities transformation. The obtained system will be approximated using an efficient and accurate spectral residual method. This method is a generalization of the spectral monic Chebyshev approximation for h-order ODEs. The obtained results are graphically represented. Various effects of different parameters, Prandtl, Lewis, Brownian motion, and thermophoresis, with the magnetic field's parameter, are reported. The reported effects on streamwise velocity, volume friction, temperature, and stream function behavior of nano-particles have been studied.

Keywords: nano-fluid, Boundary layer flow, MHD, Magnetic field, Monic Chebyshev polynomials, Spectral methods

1 Introduction

The magnetic field and its effects on a nano-fluid over a stretching sheet are significant to investigate. We have a lot of industry dependent on several effects over surface flow over a stretching layer. Some of these industries depend on the magnetic field, such as fusing metals in an electric furnace. Also, in the process of cooling the first wall inside a containment vessel of a nuclear reactor in which hot plasma is removed from the wall [1] by W. Ibrahim, B. Shankar, and M.M. Nandeppanavar. Other industries depend on many parameters in addition to a magnetic parameter such as production processes, glass-fiber processing, rubber products manufacture, extrusion, melt-spinning, etc. Furthermore, via a surrounding nano-fluid, a thin polymer layer forms a permanently dynamic surface at an irregular speed by H. S. Takhar, A.J. Chamkha, and G. Nath [2]. Experiments have shown that a stretching surface quickness is almost proportional to the distance from the nozzle by [3] J. Vlegaar.

In [4], M. Turkyilmazoglu studied how to control the momentum and heat transfers in the boundary layer flow

of various fluids over a stretching sheet by applying magnetic fields. In [5], Kumaran et al. have stated that the magnetic field makes the streamlines steeper, resulting in a thinner boundary layer. In [6], Gbadeyan et al. studied the effect of boundary layer flow of a nano-fluid past a stretching sheet with a convective boundary condition in the presence of magnetic field and thermal radiation. Hamad et al. [7] investigated the effects of the magnetic field on the free convection flow of a nano-fluid past over a vertical semi-infinite flat plate. The magnetohydrodynamic boundary layer flow of nano-fluid over an exponentially stretching permeable sheet has been investigated by K. Bhattacharyya and G. C. Layek [8]. In [9] W.A. Khan and I. Pop have investigated the nano-fluid behavior and surveyed different effects of the parameter in their paper. Hence, we will expand this study by adding an external influence, that is, the magnetic field, to study the behavior of nano-fluid.

The models that govern the fluid flow are non-linear partial and ordinary differential equations. Therefore, the need to get approximated solutions is a must. Recently, several authors investigated several methods for solving those kinds of equations [10, 11, 12, 13]. Spectral methods

* Corresponding author e-mail: mabdelhakem@yahoo.com

are considered as one of the most accurate methods that deal with the BVPs [14,15,16]. Throughout this discussion, a generalization of the spectral monic Chebyshev approximation for h-order ODEs [17] will be investigated.

The target of this work is to head our study in a meaningful direction. So, we will shed light on this study on nano-fluids that are affected by a magnetic field. This study of the influence of the magnetic field with some other simple treatments on liquids enables us to reduce a part of the costly effects. This reduction in the cost will cause a magnificence increasing in the profit. Also, the magnetic field forms a large number of our scientific studies in various areas of sciences such as mathematics, physics, and others. In addition, the effect of the magnetic field's parameter in the boundary layer over a stretched sheet embedded in a stratified medium will be studied. Other additional factors that are very important in industry, science, and engineering are included in this investigation. Moreover, each parameter affecting the flow of the nano-fluid to achieve more accuracy has been investigated. The governing PDEs are converted to third-order ODEs by the similarity transformation. Numerical calculations up to the desired degree of precision for different values of the dimensionless parameters of the problem under consideration were carried out. We will extend an accurate numerical analysis method to review the actual results of our effects. This method is the spectral monic Chebyshev's method [17].

2 Basic equations (Proposed Model)

In this section, the effect of the magnetic field on the two-dimensional boundary layers flow of nano-fluids will be discussed. Generally, through this article, the nano-fluid will be assumed to be an incompressible nano-fluid boundary layer's steady two-dimensional flow across a stretching surface with a linear velocity $u = u_w(x) = bx$, where b is a constant and x is coordinate measured along the stretching surface. The flow is estimated at $y \geq 0$, where y is the perpendicular coordinate measured to the stretching surface. It is understood that the temperature is $T = T(x,y)$ in the nano-fluid. The volume fraction of the nano-particle is $C = C(x,y)$ taking constant values at the stretching sheet T_w and C_w , respectively. T , C are the ambient values in nano-fluid, are denoted respectively by T_∞ and C_∞ . The governing equations are:

$$u_x + v_y = 0 \quad (1)$$

$$uu_x + vv_y = -\frac{P_x}{\rho} + \nu(u_{xx} + v_{yy}) - \frac{\sigma B_0^2}{\rho} u \quad (2)$$

$$uv_x + vv_y = -\frac{P_y}{\rho} + \nu(v_{xx} + v_{yy}) - \frac{\sigma B_0^2}{\rho} v \quad (3)$$

$$uT_x + vT_y = \alpha(T_{xx} + T_{yy}) + \tau \left[D_B(C_x T_x + C_y T_y) + \frac{D_T}{T_\infty} ((T_x)^2 + (T_y)^2) \right] \quad (4)$$

$$uC_x + vC_y = D_B(C_{xx} + C_{yy}) + \frac{D_T}{T_\infty} (T_{xx} + T_{yy}) \quad (5)$$

The boundary conditions are:

$$\begin{aligned} \text{at } y = 0: \\ u = u_w(x) = bx, \quad C = C_w, \quad T = T_w, \quad v = 0. \\ \text{as } y \rightarrow \infty: \\ C = C_\infty, \quad T = T_\infty, \quad u = v = 0, \end{aligned} \quad (6)$$

where:

- $u = u(x,y)$ is the velocity's component in x direction.
- $v = v(x,y)$ is the velocity's component in y direction.
- $P = P(x,y)$ is the fluid pressure coefficient.
- ρ is the density fluid coefficient.
- α is the thermal diffusivity.
- ν is the viscosity of kinematic.
- b is a positive constant.
- D_B is coefficient of the Brownian diffusion.
- D_T is coefficient of thermophoretic diffusion.
- ρ_c is the expansion coefficient of volumetric volume.
- ρ_p is the particles' density.
- $\tau = \frac{(\rho_c)_p}{(\rho_c)_f}$ is the ratio between the nano-particles material's effective heat capacity and the fluid's heat capacity with the density ρ .
- B_0 is strength of magnetic field.
- σ is Stefan-Boltzmann constant.

Consider the following similarities equations:

$$\begin{aligned} \psi = \sqrt{b\nu} x F(\eta), \quad \Theta(\eta) = \frac{T - T_\infty}{T_w - T_\infty}, \\ \Phi(\eta) = \frac{C - C_\infty}{C_w - C_\infty}, \quad \eta = \sqrt{b/\nu} y, \end{aligned} \quad (7)$$

where ψ is a stream function and typically defined as u is a partial derivative for a stream function with respect to y ($u = \frac{\partial \psi}{\partial y}$) and v is a negative partial derivative for a stream function with respect to x ($v = -\frac{\partial \psi}{\partial x}$).

By applying the similarities (7) to Eqs. (1)-(5) and the boundary conditions (6), Noted that, the outer (inviscid) flow pressure is $P = P_0$ (constant), to get:

$$F''' + FF'' - F'^2 - MF' = 0 \quad (8)$$

$$\Theta'' + PrNt \left(\Theta'^2 + \frac{F\Theta'}{Nt} + \frac{Nb}{Nt} \Theta' \Phi' \right) = 0 \quad (9)$$

$$Nt \Theta'' + Nb (\Phi'' + LeF\Phi') = 0 \tag{10}$$

subject to the boundary conditions

$$\begin{aligned} F = 0, \quad F' = 1, \quad \Theta = 1, \quad \Phi = 1 \text{ at } \eta = 0. \\ F' = 0, \quad \Theta = 0, \quad \Phi = 0 \text{ at } \eta \rightarrow \infty \end{aligned} \tag{11}$$

Where primes denote the differentiation with respect to η and the parameters are defined by:

$$\begin{aligned} Pr = \frac{v}{\alpha}, \quad M = \frac{\sigma B_0^2}{b\rho}, \quad Le = \frac{v}{D_B}, \\ Nt = \tau \frac{D_T(T_w - T_\infty)}{vT_\infty}, \\ Nb = \tau \frac{D_B(C_w - C_\infty)}{v}. \end{aligned} \tag{12}$$

Here we have some symbols for different parameters such as: M the Magnetic parameter, Pr the Prandtl number, Le the Lewis number, Nb the Brownian's motion and Nt the thermophoresis. In this analysis, the quantities of practical interest are the Nusselt number Nu and the Sherwood number Sh , which are recognized as:

$$Nu = \frac{xq_w}{k(T_w - T_\infty)}, \quad Sh = \frac{xq_m}{D_B(C_w - C_\infty)} \tag{13}$$

where q_w denote to the wall heat and q_m is the mass fluxes. Using transformation equations (7), we obtain

$$\frac{Nu}{\sqrt{Re_x}} = -\Theta'(0), \quad \frac{Sh}{\sqrt{Re_x}} = -\Phi'(0) \tag{14}$$

where Re_x is the local Reynolds number and it's value defined by $Re_x = xv^{-1}u_w(x)$ based on the stretching velocity $u_w(x)$. The reduced Nusselt number and Sherwood number are $Nur = -\Theta'(0)$ and $Shr = -\Phi'(0)$, respectively.

3 Numerical method for solving problem

The similarity transformation (7) converted the partial differential equations (1-5) with their boundary conditions (6) to an ordinary differential equations system (8-11). Due to the nonlinearity of the obtained system, the acquired systems cant be solved analytically. So, a numerical method has to be used to approximate the solution. As mentioned previously, several fluid models are approximated numerically of integer [18,19] and fractional [20] cases. Recently, many researchers have used the spectral methods because of their efficient and accurate results [21]. Some methods are dealing with h-order ODEs [17,22]. Through this work, we shall apply the standard spectral collocation method [21] or as recently colled pseudo-Garliken [23,24]. The process investigated in [17] will be our target. In this method,

Monic Chebyshev polynomials were used as the trial functions.

This method can solve linear and also nonlinear h-order BVPs. It doesn't need to reduce the order of the equations to lower ones. At the same time, it gives high accuracy in the results. Now we can represent these results graphically to clarify and discuss them.

In this method, the unknown function of the ODE "y(η)" will be represented as the spectral expansion:

$$y(\eta) = \sum_{n=0}^N a_n Q_n(\eta), \tag{15}$$

where $\phi_n(\eta); n = 0, 1, 2, \dots$ are the monic Chebyshev polynomials over the interval $[-1, 1]$ that defined in terms of Chebyshev polynomials, $T_n(\eta)$, as:

$$Q_n(\eta) = \begin{cases} 1 & , n = 0, \\ 2^{1-n} T_n(\eta) & , n \geq 1. \end{cases} \tag{16}$$

For more details about Chebyshev and monic Chebyshev polynomials in several domains that that reader may need, kindly refer to [17,24,25].

Now, shift the domain of the Eqs. (8-10) and its boundary conditions (11) to the Monic Chebyshev polynomials' domain using any suitable transformation. According to the expansion (15), let:

$$F(\eta) = \sum_{n=0}^N \beta_n Q_n(\eta), \tag{17}$$

$$\Theta(\eta) = \sum_{n=0}^N \gamma_n Q_n(\eta), \tag{18}$$

$$\Phi(\eta) = \sum_{n=0}^N \delta_n Q_n(\eta). \tag{19}$$

Substitute from equations (17-19) into the system of ordinary equations, after the shitting , to get a system of algebraic equations. This system can be solved by any solver to to get the unknowns β_n, γ_n and δ_n .

4 Results and discussion

The influence of a magnetic field on the behaviour of nano-fluids will be explored in this paper. The influence and modification of the nano-fluid will be noted for many parameters such as the Prandtl number, Lewis number, Brownian motion parameter, thermophoresis parameter, and so on. The expression of "nano-fluid behaviour," that is, the influence of various parameters on temperature, nano-particle volume fraction, and streamwise velocity, is well recognized. In the beginning, it showed the effect of the first parameter on which our research paper is based, the magnetic field. Figure (1) shows the effect for

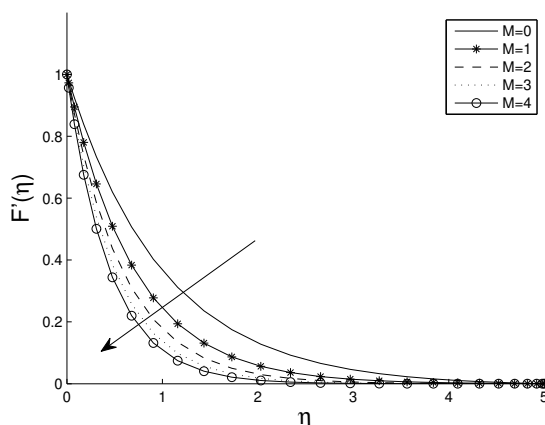


Fig. 1: Effectiveness M over $F'(\eta)$ with η when $Pr = Le = 1, Nb = Nt = 0.1$.

different values of magnetic parameters over the streamwise velocity $F'(\eta)$ at $Pr = Le = 1, Nb = Nt = 0.1$, and $M = 0, 1, 2, 3, 4, 5$. The magnetic field resists the streamwise velocity and transport process. In fact, increasing M contributes to the growth of Lorentz's strength. It is known about Lorentz's force and what we do to measure it generated in a moving nanofluid due to exposure to a changing magnetic field. Whereas, according to Faraday's law, when a conducting metal or liquid moves within a magnetic field, induced currents called eddy currents are generated; these currents, in turn, generate secondary magnetic fields according to Ampere's and Maxwell's law. The interaction of eddy currents with secondary magnetic fields generates Lorentz forces that oppose the direction of movement of the nanofluid or the carrier metal and impede its movement. According to Newton's third law (law of action and reaction), a force equal to the Lorentz force is generated with an amplitude and opposite direction that affects the main magnetic field. This body force decelerates the boundary layer flow, thickens the momentum boundary layer, and hence increases the absolute value of the velocity gradient at the surface. We will find more significant opposition to the transport phenomenon through Lorentz's greater force. Therefore, the magnetic field reduces the velocity of the nano-fluid. It's clear that the streamwise velocity $F'(\eta)$ doesn't be affected by the parameters Pr, Le, Nb , and Nt as showed in Figure (22), the Prandtl number effectiveness with the constants $M = Le = 1, Nb = Nt = 0.1$, and $Pr = 1, 2, 4$.

In figures (2) and (3), $Pr = Le = 1, Nb = Nt = 0.1$, and $M = 0, 1, 2, 3, 4, 5$, the effect of the magnetic field was studied on both the temperature and the size of the nano-particle fraction. That found the temperature was getting high, and it seemed that Lorentz's strength had a hand in this. So we increased the scrutiny and found that due to Lorentz's force, it works to slow down and reduce

the nano-fluid's movement and increases its resistance. We can say this is the reason to increases the temperature rise. Consequently, the temperature is directly proportional to the magnetic field. This also affects the size of the nano-particle fraction, which increases the thickness of the boundary layer.

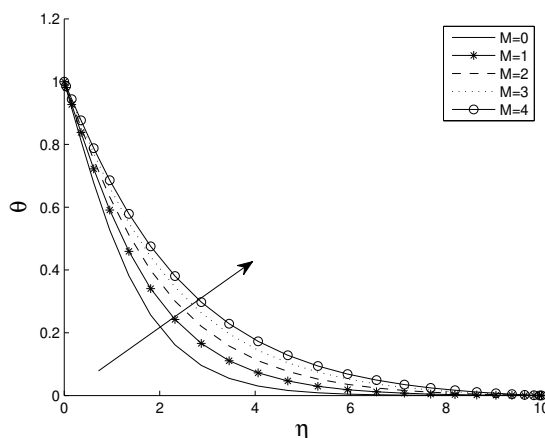


Fig. 2: Effectiveness of M over $\Theta(\eta)$ with η when $Pr = Le = 1, Nb = Nt = 0.1$.

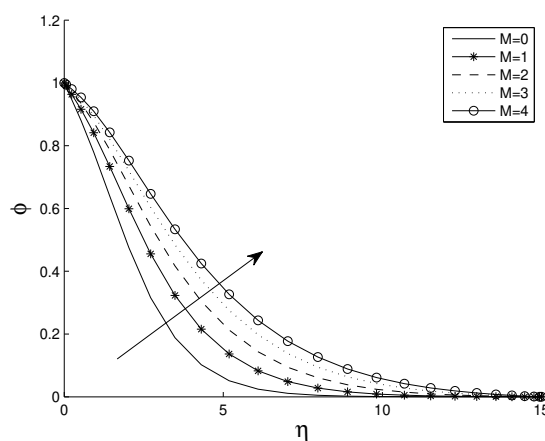


Fig. 3: Effectiveness of M over $\Phi(\eta)$ with η when $Pr = Le = 1, Nb = Nt = 0.1$.

In Figures (4) and (5) with $M = 2, Le = 1, Nb = Nt = 0.1$, and $Pr = 2, 4, 6, 8, 10$, the effects of Prandtl number Pr on the temperature and nanoparticles volume fraction are represented. It's clear that the prandtl number is inversely proportional to the thermal boundary layer thickness and thermal diffusivity. For large values of

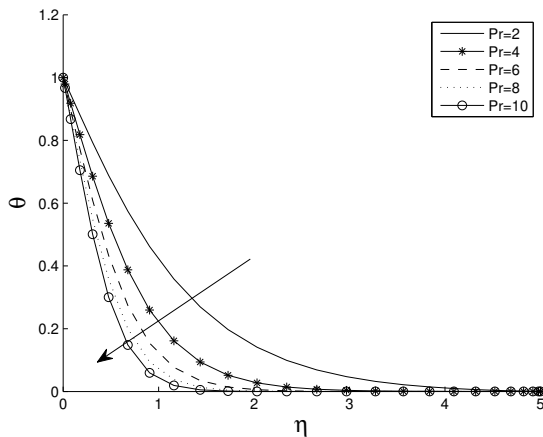


Fig. 4: Effectiveness of Pr over $\Theta(\eta)$ with η when $Le = 1$, $Nb = Nt = 0.1$, $M = 2$.

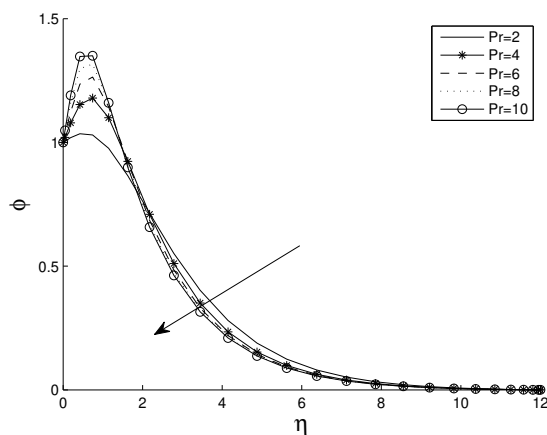


Fig. 5: Effectiveness of Pr over $\Phi(\eta)$ with η when $Le = 1$, $Nb = Nt = 0.1$, $M = 2$.

Pr , the nano-particles' volume fraction surpasses near the sheet. The diameter of the nano-particles' volume boundary layer decreases. Therefore, the nano-particles' volume fraction $\Phi(\eta)$ is higher in the fluid adjacent to the sheet than the value at the wall for higher values of Prandtl number with zero rate of change for thermophoretic particle deposition.

The effect of Nb is reviewed on the nano-particles' fluid temperature and the fraction size. It is clear that the size of the fraction in the nano-particles is inversely proportional to the Nb . increases, we found a lot of decrease in the fraction size of the nano-particles. That is reflected in the nano-particles' volume boundary layer thickness decreases where it also decreases. The Brownian movement takes place in the nano-fluids system due to the presence of nano-particles, and the Brownian

motion is caused by the increase in Nb and, therefore, the fluid changes characteristic of heat transfer. All this is illustrated in Figures (6) and (7) when $M = Pr = Le = 1$, $Nt = 0.1$, and $Nb = 0.2, 0.4, 0.7, 1, 1.3$.

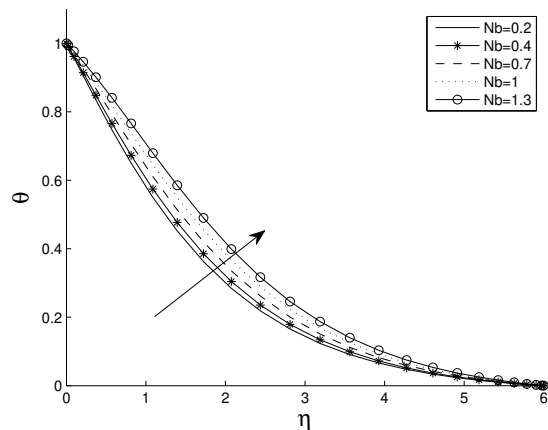


Fig. 6: Effectiveness of Nb over $\Theta(\eta)$ with η when $Pr = Le = M = 1$, $Nt = 0.1$.

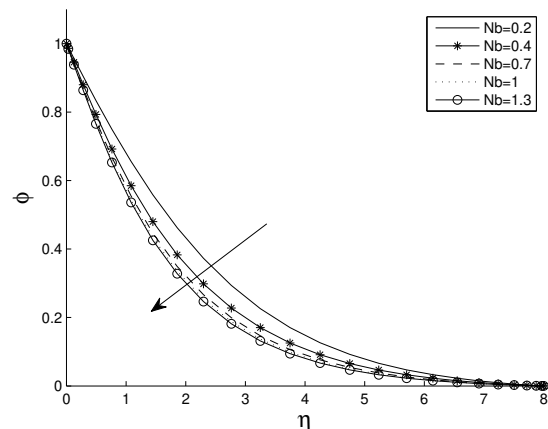


Fig. 7: Effectiveness of Nb over $\Phi(\eta)$ with η when $Pr = Le = M = 1$, $Nt = 0.1$.

The Nt thermophoresis parameter is a crucial parameter for the analysis of temperature allocation and volume fraction of nano-particles in nano-fluids flow. In Figures (8) and (9), $M = Le = 1$, $Nb = 0.1$, and $Nt = 0.2, 0.3, 0.5, 0.8, 1$, the effect of the thermophoresis parameter Nt is shown on the temperature $\Theta(\eta)$ and the volume fraction of the nano-particles $\Phi(\eta)$. If Nt rises, the temperature of the fluid rises also. The nano-particles'

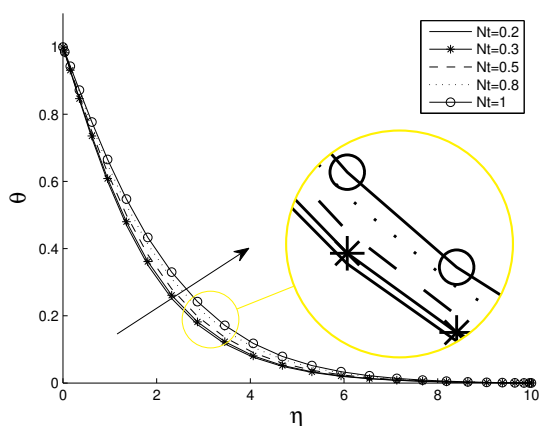


Fig. 8: Effectiveness of Nt over $\Theta(\eta)$ with η when $Pr = Le = M = 1, Nb = 0.1$.

volume fraction directly proportional to Nt . We note that the overshoot is happened located near the wall. Rising Nt enables the intensity of thermophoresis to increase. It's known that is any material tends to move from hot areas to more minor hot spots (meaning more precisely to cold places). It is the same happened with nano-particles is moving from hot to cold spots. This raises the magnitude of nano-particles temperature performance and fractional volume performance. At last, the thickness of the nano-particles volume boundary layer gets extraordinarily high for a little rising value of the thermophoresis parameter.

After our study of this proposed model, we found that the local Nusselt number Nu and the local Sherwood number Sh also affect the behavior of the nano-fluid. Some of their effects are presented as an example, but not a limitation. Different values of $M, Pr, Le, Nb, Nt, -\Theta'(0)$, and $-\Phi'(0)$ are plotted in Figures (10-21) for various values of the parameters.

The value of the local Nusselt number and the local Sherwood number is represented in Figure (10-13) with various magnetic parameter values, $M = 0, 1, 2, 3$, and fixed parameters values $Pr = Le = 1, Nt = 0.1$, and $Nb = 0.1$. When the magnetic field increases and is more robust, both the local Nusselt number and the local Sherwood are affected by this increase in the opposite way. Also, the values of $-\Theta'(0)$, and $-\Phi'(0)$ are depicted against the Brownian motion parameter Nb and the thermophoresis parameter Nt for various values of M in Figures (10) to (13).

Another graph that established the substantial Lorentz force that resulted in a flow field for a significant magnetic field decreases the values of the local Nusselt number and the local Sherwood number.

With the changeability of the other parameters, the effect of the Prandtl number Pr with the different values

($Pr = 1, 2, 4$) and Lewis number Le with the various values ($Le = 0.5, 1, 2$) on the local Nusselt number Nu and the local Sherwood number Sh are shown in Figures (14) to (21). It is obvious to note that, the Prandtl number is directly proportional to the local Nusselt number and inversely proportional to the local Sherwood number.

When the Prandtl number rises, so does the heat transfer rate. There is a difference between the Prandtl number and Lewis number effects; because Their effects are entirely opposite to each other over the Nusselt number and Sherwood number. The Lewis number affects the Nusselt number (reduction) and the Sherwood number (increment).

For small values of the Lewis number, the Brownian diffusion effect is significant, and accordingly, the increased heat transfer rate is found (more significant Nusselt number, Figure (18)). Figures (10) to (21) show the changes in the local Nusselt and Sherwood numbers for the Brownian motion parameter Nb and the thermophoresis parameter Nt . For a high rate of the Brownian motion, that is, for increasing Nb , the values of $-\Theta'(0)$ reduce, and those of $-\Phi'(0)$ increase. But the increase in the thermophoresis parameter Nt causes a reduction in both, the local Nusselt number and the local Sherwood number.

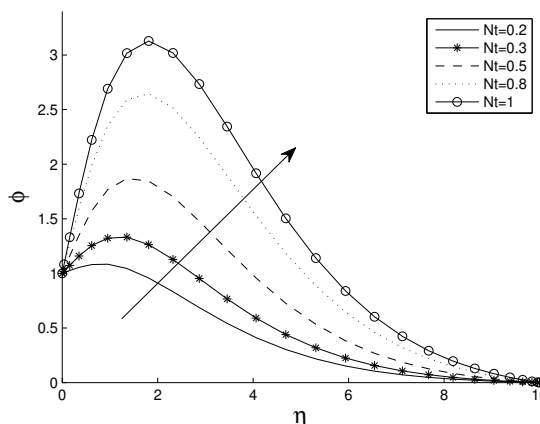


Fig. 9: Effectiveness of Nt over $\Phi(\eta)$ with η when $Pr = Le = M = 1, Nb = 0.1$.

5 Conclusions

In this work, the effects of the magnetic field on nano-fluids have been studied. Similarity equations transform the nano-fluid's movement equations system and the boundary conditions to a system of ODEs. That system can be solved numerically using a spectral method based on monic Chebyshev polynomials. This numerical

Table 1: symbols

u & v	Component of velocity in x, y directions	∞	Condition at the free stream
C_w	nanoparticle volume fraction at the stretching surface	w	Condition at the wall
C_∞	ambient nanoparticle volume fraction	0	Condition at the initial
C	Nanoparticles volume fraction	x	derivative with respect to coordinate along the sheet
D_T	thermophoretic diffusion coefficient	y	derivative with respect to coordinate perpendicular to the sheet
D_B	Brownian diffusion coefficient		
$F(\eta)$	dimensionless Streamwise function		
Le	Lewis number		
Nb	Brownian motion parameter		
Nt	thermophoresis parameter		
Nu	Nusselt number		
Pr	Prandtl number		
T_w	temperature at the stretching surface		
T	temperature		
T_∞	Ambient temperature		
Re_x	local Reynolds number		
u_w	velocity of the stretching sheet		
b	Positive integer constant		
P	Pressure		
			<i>* Greek symbols *</i>
		η	similarity variable
		$\Theta(\eta)$	dimensionless temperature
		$\Phi(\eta)$	rescaled nanoparticle volume fraction
		ψ	stream function
		ρ	density of the fluid
		σ	Stefan-Boltzmann constant
		α	thermal diffusivity

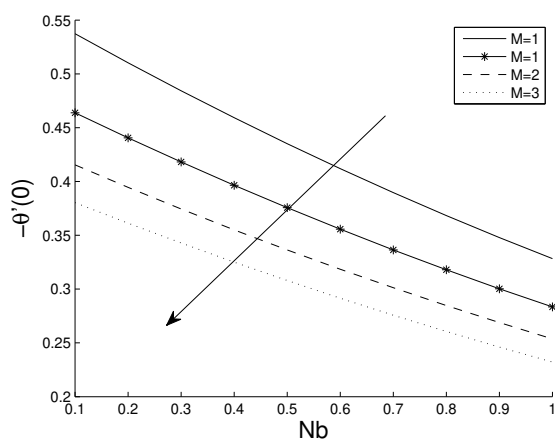


Fig. 10: Variation of $-\Theta'(0)$ with Brownian motion parameter Nb when $Pr = Le = 1, Nt = 0.1$.

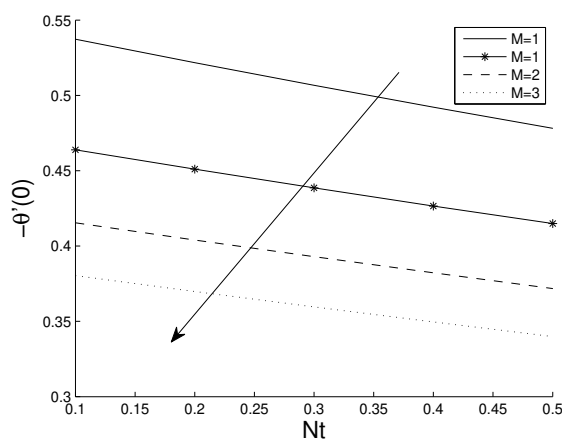


Fig. 11: Variation of $-\Theta'(0)$ with thermophoresis parameter Nt when $Pr = Le = 1, Nb = 0.1$.

method has proven its effectiveness in solving our system of equations with high accuracy. Several graphs present the results to facilitate visualization of the effects on the nano-fluid. The model used for the nano-fluid incorporates the effects of the magnetic field, Brownian motion, and thermophoresis. The ODEs are presented, which depend on $M, Pr, Le, Nb,$ and Nt . A significant change in the behavior of nano-fluid has been observed; the most important of this with the rising magnetic field, transport rates are decreasing, raising on temperature, and increasing the thickness of the boundary layer.

Acknowledgment

The authors would like to thank the anonymous reviewers for carefully reading the article and also for their constructive and valuable comments, which have improved the paper in its present form. The authors are also sincerely grateful to the Helwan School of Numerical Analysis in Egypt (HSNAE) members for their valuable support during this research.

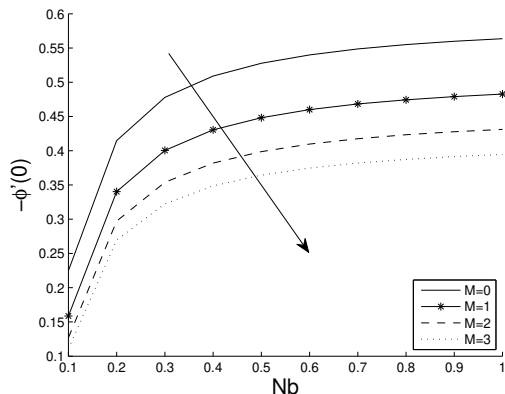


Fig. 12: Variation of $-\Phi'(0)$ with Brownian motion parameter Nb when $Pr = Le = 1, Nt = 0.1$.

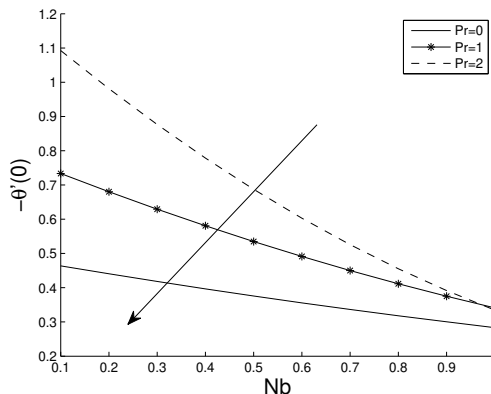


Fig. 14: Variation of $-\Theta'(0)$ with Brownian motion parameter Nb when $M = Le = 1, Nt = 0.1$.

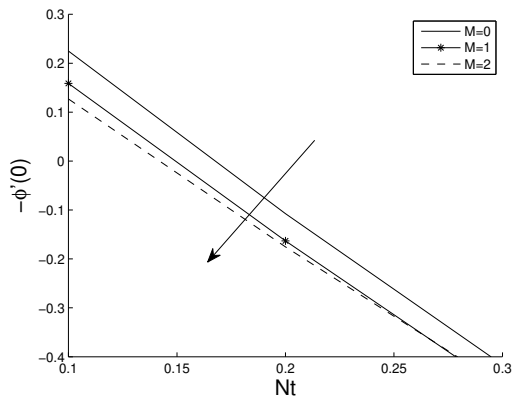


Fig. 13: Variation of $-\Phi'(0)$ with thermophoresis parameter Nt when $Pr = Le = 1, Nb = 0.1$.

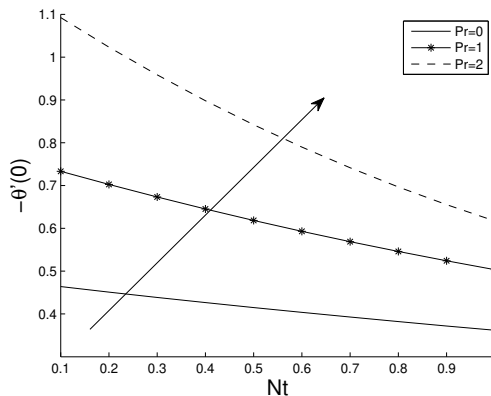


Fig. 15: Variation of $-\Theta'(0)$ with thermophoresis parameter Nt when $M = Le = 1, Nb = 0.1$.

Conflict of interest

The authors declare that they have no conflict of interest.

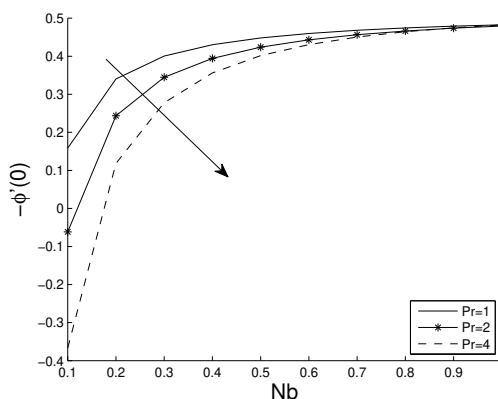


Fig. 16: Variation of $-\Phi'(0)$ with Brownian motion parameter Nb when $M = Le = 1, Nt = 0.1$.

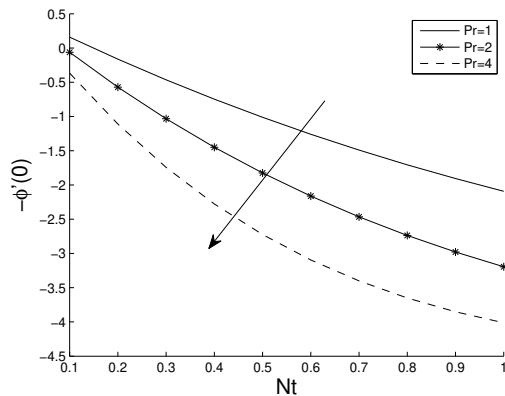


Fig. 17: Variation of $-\Phi'(0)$ with thermophoresis parameter Nt when $M = Le = 1, Nb = 0.1$.

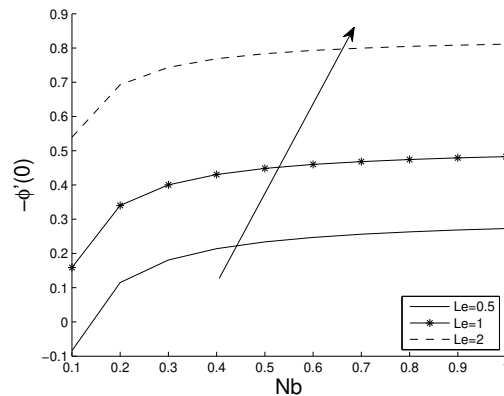


Fig. 20: Variation of $-\Phi'(0)$ with Brownian motion parameter Nb when $M = Pr = 1, Nt = 0.1$.

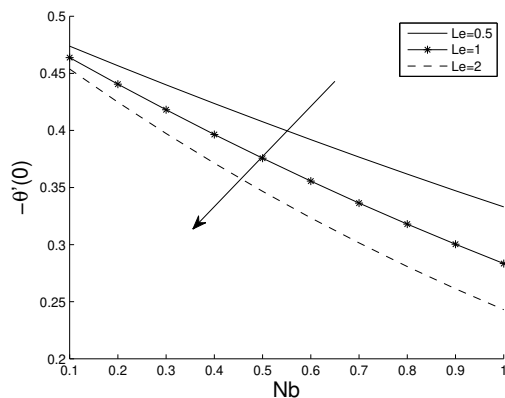


Fig. 18: Variation of $-\Theta'(0)$ with Brownian motion parameter Nb when $M = Pr = 1, Nt = 0.1$.

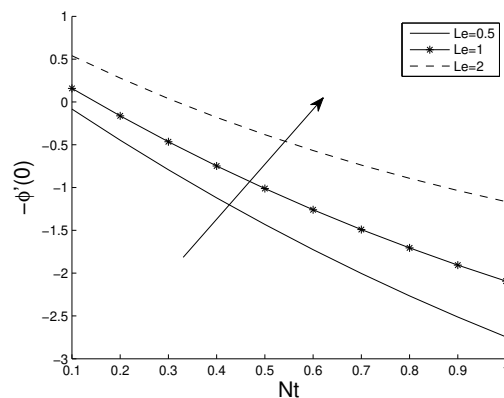


Fig. 21: Variation of $-\Phi'(0)$ with thermophoresis parameter Nt when $M = Pr = 1, Nb = 0.1$.

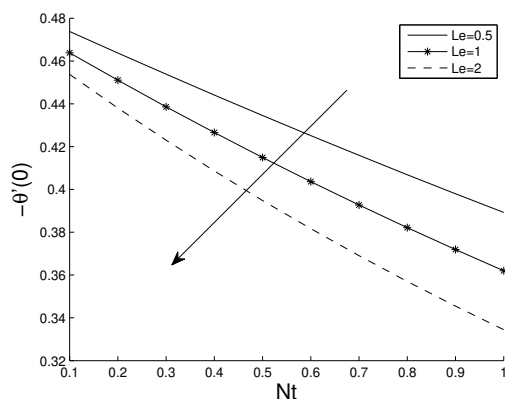


Fig. 19: Variation of $-\Theta'(0)$ with thermophoresis parameter Nt when $M = Pr = 1, Nb = 0.1$.

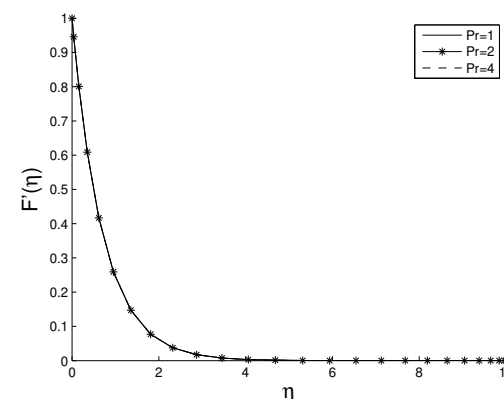
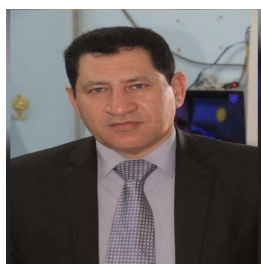


Fig. 22: Effectiveness of Pr over $F'(\eta)$ with η when $M = Le = 1, Nb = Nt = 0.1$.

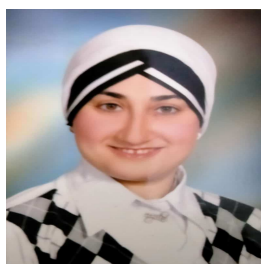
References

- [1] W. Ibrahim, B. Shankar, M.M. Nandeppanavar, MHD stagnation point flow and heat transfer due to nanofluid towards a stretching sheet, *Int. J. Heat Mass Transf.*, **56**(1-2), 1-9 (2013).
- [2] H.S. Takhar, A.J. Chamkha, G. Nath, Unsteady three-dimensional MHD-boundary-layer flow due to the impulsive motion of a stretching surface, *Acta Mechanica*, **146**, 59-71 (2001).
- [3] J. Vlegaar, Laminar boundary-layer behaviour on continuous, accelerating surfaces, *Chem. Eng. Sci.*, **32**(12), 1517-1525 (1977).
- [4] M. Turkyilmazoglu, Exact analytical solutions for heat and mass transfer of MHD slip flow in nanofluids, *Chem. Eng. Sci.*, **84**, 182-187 (2012).
- [5] V. Kumaran, A.K. Banerjee, A.V. Kumar, K. Vajravelu, MHD flow past a stretching permeable sheet, *Appl. Math. Comput.* **210**(1), 26–32 (2009).
- [6] J.A. Gbadeyan, M.A. Olanrewaju, P.O. Olanrewaju, Boundary layer flow of a nanofluid past a stretching sheet with a convective boundary condition in the presence of magnetic field and thermal radiation, *Australian Journal of Basic and Applied Sciences*, **5**(9), 1323-1334 (2011).
- [7] M.A.A. Hamad, I. Pop, A.I.M. Ismail, Magnetic field effects on free convection flow of a nanofluid past a vertical semi-infinite flat plate, *Nonlinear Anal.-Real World Appl.*, **12**(3), 1338–1346 (2011).
- [8] K. Bhattacharyya, G.C. Layek, Magnetohydrodynamic boundary layer flow of nanofluid over an exponentially stretching permeable sheet, *Phys. Res. Int.*, **2014**, 592536 (2014).
- [9] W.A. Khan, I. Pop, Boundary-layer flow of a nanofluid past a stretching sheet, *Int. J. Heat Mass Transf.*, **53**(11-12), 2477–2483 (2010).
- [10] J. Shahni, R. Singh, Bernstein and Gegenbauer-wavelet collocation methods for Bratu-like equations arising in electrospinning process. *J. Math. Chem.*, **2021**, 1-17 (2021).
- [11] O.Nikan, J.A.T. Machado, A.Golbabai, J. Rashidinia, Numerical evaluation of the fractional Klein–Kramers model arising in molecular dynamics, *J. Comput. Phys.*, **428**(1), 109983 (2021).
- [12] O.Nikan, Z. Avazzadeh, J.A.T. Machado, Numerical approximation of the nonlinear time-fractional telegraph equation arising in neutron transport, *Commun. Nonlinear Sci. Numer. Simul.* **99**, 105755 (2021).
- [13] M. Alghamdi, A. Wakif, T. Thumma, U. Khan, D. Baleanu, G. Rasool, Significance of variability in magnetic field strength and heat source on the radiative-convective motion of sodium alginate-based nanofluid within a Darcy-Brinkman porous structure bounded vertically by an irregular slender surface, *Case Stud. Therm. Eng.* **28**, 101428 (2021).
- [14] Y.H. Youssri, W.M. Abd-Elhameed, M. Abdelhakem, A robust spectral treatment of a class of initial value problems using modified Chebyshev polynomials, *Math. Meth. Appl. Sci.*, **44**(11), 9224-9236 (2021).
- [15] M. Abdelhakem, D. Abdelhamied, M.G. Alshehri, M. El-Kady, Shifted Legendre fractional pseudospectral differentiation matrices for solving fractional differential problems, *Fractals*, **30**(1), 2240038 (2022).
- [16] A.K. Dizicheh, S. Salahshour, A. Ahmadian, D. Baleanu, A novel algorithm based on the Legendre wavelets spectral technique for solving the Lane–Emden equations, *Appl. Numer. Math.*, **153**(1), 443-456 (2020).
- [17] M. Abdelhakem, A. Ahmed and M. El-kady. *Spectral monic Chebyshev approximation for higher order differential equations. Math. Sci. Lett.*, **8**(2), 11-17 (2019).
- [18] G.A. Danish, M. Imran, M. Tahir, H. Waqas, M.I. Asjad, A. Akgül, D. Baleanu, D., Effects of non-linear thermal radiation and chemical reaction on time dependent flow of Williamson nanofluid with combine electrical MHD and activation energy. *J. Appl. Comput. Mech.*, **7**(2), 546-558 (2021).
- [19] M.R. Eid, K. Mahny, A. Dar, T. Muhammad, Numerical study for Carreau nanofluid flow over a convectively heated nonlinear stretching surface with chemically reactive species, *Physica A*, **540**, 123063 (2020).
- [20] U. Farooq, H. Khan, F. Tchier, E. Hincal, D. Baleanu and H. B. Jebreen, New approximate analytical technique for the solution of time fractional fluid flow models, *Adv. Differ. Equ.*, **2021**, 81 (2021).
- [21] M. Abdelhakem, Y.H. Youssri, Two spectral Legendre's derivative algorithms for Lane-Emden, Bratu equations, and singular perturbed problems, *Appl. Numer. Math.*, **169**, 243-255 (2021).
- [22] M. Abdelhakem, M. Biomy, S. Kandil, D. Baleanu, M. El-kady, A numerical method based on Legendre differentiation matrices for higher order ODEs, *Inf. Sci. Lett.*, **9**(3), 175-180 (2020).
- [23] M. Abdelhakem, T. Alaa-Eldeen, D. Baleanu, Maryam G. Alshehri, M. El-kady, Approximating real-life BVPs via Chebyshev polynomials' first derivative Pseudo-Galerkin Method, *Fractal Fract.*, **5**(4), 165 (2021).
- [24] M. Abdelhakem, D. Mahmoud, D-Baleanu, M. El-kady, Shifted Ultraspherical pseudo-Galerkin method for approximating the solutions of some types of ordinary fractional problems, *Adv. Differ. Equ.*, **2021**, 110 (2021).
- [25] M. Abdelhakem, H. Moussa, D. Baleanu, M. El-Kady, Shifted Chebyshev schemes for solving fractional optimal control problems, *J. Vib. Control* **25**(15) (2019) 2143-2150.



Emad M. Abo-Eldahab
Professor Emad M. Abo-Eldahab graduated from Helwan University, Cairo, Egypt, in 1987. He received the M. Sc. degree in mathematics from Helwan University, Cairo, Egypt, in 1993, and the Ph. D. degree in applied mathematics from

Helwan University, Cairo, Egypt, in 1997. He is the former head of the mathematics department, Helwan University, Cairo, Egypt. Now, he is the dean of the faculty of Science, Helwan University, Cairo, Egypt. His research interests are focused on fluid mechanics. He published numerous papers in fluid mechanics.



Rasha Adel graduated from Helwan University, Cairo, Egypt, in 1999. She received the M. Sc. degree in mathematics from Helwan University, Cairo, Egypt, in 2007, and the Ph. D. degree in applied mathematics from Helwan University, Cairo, Egypt, in 2012. Her research

interests are focused on fluid mechanics.



Hoda Mubarak received her Bachelor's degree from the mathematics department, faculty of Science, Helwan University, Egypt in Mathematics in 2016. She prepares a master's degree in Applied Mathematics from the same university. Her research interests are focused

on fluid mechanics.



Mohamed Abdelhakem graduated from Helwan University, Cairo, Egypt, in 1999. He received the M. Sc. degree in Computer Science from Helwan University, Cairo, Egypt, in 2003, and the Ph. D. degree in pure mathematics from Helwan University, Cairo, Egypt, in

2011. He is the Vice-Chairman and founder of Helwan School of Numerical Analysis in Egypt "HSNAE". His research interests in numerical analysis and optimal control. He is a reviewer in several international journals.